Quantum Information Processing (2023) 22:220
https://doi.org/10.1007/s11128-023-03961-y

Swap Test-based characterization of decoherence in universal quantum computers

Pedro Ripper[1] · **Gustavo Amaral**[1,2] · **Guilherme Temporão**[1,3]

Received: 5 February 2022 / Accepted: 24 April 2023 / Published online: 17 May 2023

Abstract
Unreliable quantum processes stemming from noisy operations and interactions with the environment represent one of the greatest challenges to be overcome in the development of scalable, fault-tolerant universal quantum computers. Generic characterizations of such quantum processes, however, can be very resource-intensive, and many tools have been developed for identifying particular aspects of a quantum computer. In this article, we verify whether a tool called Swap Test can be used in order to identify decoherence in an implementation-agnostic way. Simulations and experimental results show that a modified version of a Toffoli Swap Test can be employed as an alternative to a full quantum process tomography, consuming considerably less computational resources as a consequence. Moreover, it is also shown to be able to simulate in a generic quantum computer a quantum optical communication link that employs two-photon interference.

Keywords Quantum computing · Quantum process · Quantum decoherence · Swap Test

1 Introduction

Quantum computing has been gaining traction among other technologies that will revolutionize our future. The expectation that quantum computers will harness what is

✉ Pedro Ripper
pripper@opto.cetuc.puc-rio.br

Gustavo Amaral
gustavo.castrodoamaral@tno.nl

Guilherme Temporão
temporao@opto.cetuc.puc-rio.br

1 Pontifical Catholic University of Rio de Janeiro, Rio de Janeiro 22459-900, Brazil

2 The Netherlands Organization for Applied Scientific Research, Delft 2628CK, The Netherlands

3 Department of Electrical Engineering PUC-Rio, Rio de Janeiro 22459-900, Brazil

known as *Quantum Speedup* has recently placed this field under the spotlight, which attracted huge investments from both governmental and private sectors. Yet, we are in a stage of quantum computing called NISQ era [1] that is characterized by quantum computers that are still very vulnerable to unreliable operations and decoherence by interactions between its system and the environment. Much has been done in the field for characterizing quantum computers' performance [2, 3] amid these shortcomings, such as randomized benchmarking [4–6] for gate fidelity estimation and quantum volume [7] evaluation for a more general metric about a quantum computers's performance. Concerning individual quantum gates, well-established techniques of quantum state tomography and quantum process tomography [8, 9] can be employed, which usually rely on repeatedly measuring a series of predetermined observables. However, these routines are overly costly on the Hilbert space dimension and are seldom employed in practice; most approaches take into advantage some property of the physical system being considered, such as compressed sensing tomography [10], scalable tomography [11], algorithms based on machine learning [12] and specially tailored techniques for Clifford gates [13–15]. No one of these methods, however, is exclusively interested in determining decoherence effects, and therefore use more resources than needed for the sole purpose of decoherence estimation.

Quantum decoherence has also been a topic of study outside the context of quantum computing. In the framework of quantum optical communication, for example, depolarization effects can lead to decoherence whenever the polarization degree of freedom is employed for encoding quantum information [16]. In a previous work by our group [17], we have shown how two-photon interference in a Hong-Ou-Mandel (HOM) interferometer [18] can be exploited in order to determine whether decoherence has taken place. However, the HOM phenomenon is an effect restricted to the context of photonics. Aiming for a device-agnostic framework, we employ the Swap Test (ST) [19] as an alternative, due to the fact that it has been proven equivalent to the HOM effect for input pure states [20]. The ST has been employed in different contexts, such as variational quantum algorithms [21], pattern recognition [22] and entanglement spectroscopy [23] and has been experimentally implemented in quantum dot charge qubits [24], photonic circuits [23], trapped ions [25] and superconducting platforms [26].

Here, we propose a ST-based methodology to characterize an unknown quantum process or an unknown qubit with varying purity from 0 (completely mixed) to 1 (pure), irrespective of the quantum computer architecture. We also present the outcomes from our research from previous works about the ST [19, 20, 27, 28] followed by shortcomings of this technique. Yet, as will be shown in this work, the standard ST setting is not able to completely characterize a qubit in a mixed state. Therefore, we propose adjustments to the current ST protocol, in order to check whether a qubit has been affected by decoherence or, rather, a random unitary operation—see Fig. 1. All the herewith presented experiments were conducted using IBM's Qiskit [29] framework to simulate quantum circuits and execute them on real quantum computers.

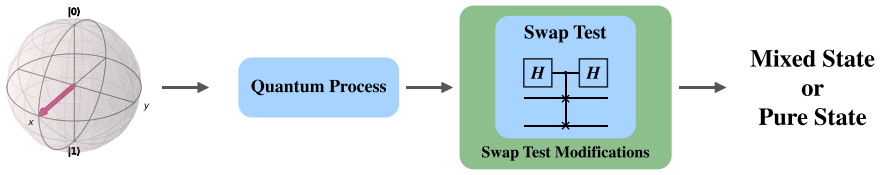

Fig. 1 Motivation: using the Swap Test to check for a possible decoherence process that an unknown qubit could have undergone. The output of the process should identify the input state as a mixed or pure state without the need for complete quantum state tomography

2 The Swap Test

The impossibility of deterministically distinguishing between two general unknown quantum states is one of the core features of quantum mechanics [30]. Therefore, methods that provide information on how close two quantum states $|\phi\rangle$ and $|\psi\rangle$ are from one another - such as the *fidelity* $F = |\langle\psi|\phi|\rangle|^2$ - must be probabilistic. For example, one can verify whether two qubits are identical to each other by projecting their joint state onto the singlet two-qubit state $|\psi^-\rangle = \frac{1}{\sqrt{2}}(|0\rangle|1\rangle - |1\rangle|0\rangle)$, where $\{|0\rangle, |1\rangle\}$ represent the computational basis elements of a single-qubit Hilbert space. Indeed, it is easy to show that

$$\langle\psi^-|\phi||\psi\rangle = 0 \iff |\psi\rangle = |\phi\rangle \tag{1}$$

which means that a full Bell-state measurement (BSM) has zero probability of producing an outcome associated to the singlet state if the two qubits are identical. Therefore, by repeating the experiment multiple times, it is possible to determine, up to an arbitrarily high degree of confidence, whether two input states are identical or not. It is important to note that even a single measurement can provide information: If the projection onto the singlet state is successful, than one can predict with certainty that the input states have fidelity strictly less than one. In the case of many qubits, more advanced algorithms have been proposed to obtain the fidelity in an efficient manner [31].

However, the projection onto the singlet state has some limitations; one of them is that it is a destructive procedure. Even if the two input states are identical, they are destroyed in the process. Introduced by Buhrman et al under the context of quantum fingerprinting [19], the *Swap Test* (ST) is a class of methods that can also distinguish between two quantum states $|\phi\rangle$ and $|\psi\rangle$, with the advantage of being able to not destroy the states (by employing an ancilla qubit). There are different variations of quantum circuits that are capable of realizing the operation known as the Swap Test. In our work, we focused on two, that we shall call the Controlled-Swap (CSWAP) ST, which is of the nondestructive kind, and the Bell-state measurement (BSM) ST, which is very close to the projection onto the singlet state shown above.

The CSWAP ST is comprised of three qubits. The first one is an ancillary qubit, initially in the $|0\rangle$ state. The other qubits, $|\phi\rangle$ and $|\psi\rangle$, are the ones which will have their states compared. In the circuit, firstly, a Hadamard operator is applied on the ancillary qubit. In the Controlled-Swap gate that follows, the ancilla acts as a control

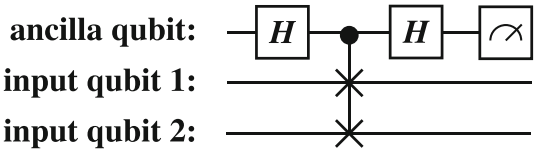

Fig. 2 Controlled-Swap (CSWAP) ST circuit

qubit, whereas the Swap gate targets the remaining states. Finally, the ancilla qubit is measured after a second Hadamard operation (which is equivalent to measuring in the Hadamard basis). The CSWAP ST circuit is portrayed in Fig. 2 and its operations unfold as shown in Eq. 2.

$$\begin{aligned} |0\rangle|\psi\rangle|\phi\rangle &\xrightarrow{H} \frac{|0\rangle+|1\rangle}{\sqrt{2}}|\psi\rangle|\phi\rangle \xrightarrow{CSWAP} \frac{|0\rangle|\psi\rangle|\phi\rangle+|1\rangle|\phi\rangle|\psi\rangle}{\sqrt{2}} \\ &\xrightarrow{H} \frac{\frac{|0\rangle+|1\rangle}{\sqrt{2}}|\psi\rangle|\phi\rangle+\frac{|0\rangle-|1\rangle}{\sqrt{2}}|\phi\rangle|\psi\rangle}{\sqrt{2}} \\ &\rightarrow \frac{|0\rangle(|\psi\rangle|\phi\rangle+|\phi\rangle|\psi\rangle)+|1\rangle(|\psi\rangle|\phi\rangle-|\phi\rangle|\psi\rangle)}{2} \end{aligned} \tag{2}$$

Following the operations, a measurement is performed on the ancillary qubit, and according to Eq. 3, two outcomes are possible. First, if states $|\phi\rangle$ and $|\psi\rangle$ are indistinguishable, $|0\rangle$ is found with a 100% probability. On the other hand, if they are distinct, both $|0\rangle$ and $|1\rangle$ are possible outcomes, with a specific probability which can be estimated, given by Eq. 3.

$$\begin{aligned} P(|0\rangle) &= \frac{(\langle\psi|\langle\phi|+\langle\phi|\langle\psi|)(|\psi\rangle|\phi\rangle+|\phi\rangle|\psi\rangle)}{4} \\ P(|0\rangle) &= \frac{2\langle\psi|\phi|^2+2}{4} = \frac{\langle\psi|\phi|^2+1}{2} \\ P(|1\rangle) &= 1-P(|0\rangle) = \frac{1-\langle\psi|\phi|^2}{2} \end{aligned} \tag{3}$$

Consequently, in order to find whether two states are equal, it would be necessary to realize several iterations of the ST with no occurrences of the outcome 1. On the other hand, a single result 1 from the ST would be sufficient to prove that the states are distinguishable. Such circumstances show that a single outcome 0 from the ST does not give any real information about the input qubits, leaving the ST attempt inconclusive.

The CSWAP ST circuit, previously presented in Fig. 2, has been offered some modifications on different articles [20, 27], being the BSM ST one of them. Although there were no changes in the probability distribution of outcomes between the CSWAP and BSM ST, the latter arrangement provides a significant modification: the BSM ST does not need an ancilla qubit as the CSWAP ST, as presented in Fig. 3. The final result from the BSM ST is "1" if both qubits are measured in the state $|1\rangle$, which corresponds to a logical AND gate. Any of the other possible measurements yields

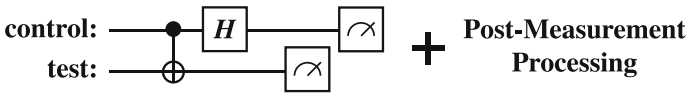

Fig. 3 Bell-state measurement Swap Test (BSM ST) circuit. The post-measurement processing corresponds to a logical AND gate between the measurement outputs

"0" for the final outcome. Despite of the lack of an ancilla and the additional post-measuring processing, the BSM ST probabilities of output follow the ones from the CSWAP ST.

It should be pointed out that the usage of the ST for fidelity estimation was designed for qubits in *pure* states. With that in mind, in this paper we present a ST attempt for a qubit in a mixed state with another in a pure state. As will be seen, the ST is unable to perform such comparison and requires an adaptation, which will be presented in Sect. 3, that makes possible to identify whether a qubit is in a mixed state.

2.1 Characterization methodology with the Swap Test

As our main goal was to obtain more information about a qubit in a "unknown" state by detecting whether it has suffered decoherence or not, we established that it would be used as an input for the ST alongside another qubit in a "known" (pure) state.

The proposed scheme consists in comparing a known pure state with an unknown (pure or mixed) state, henceforth identified as the *control* and *test* qubits, respectively. These states are prepared according to the scheme depicted in Fig. 4. The *control* qubit, being a pure state, can be prepared by a single one-qubit gate representing a general unitary operation U_{ctrl}; however, the *test* qubit requires a slightly more complicated setup as it can be in a mixed state. A mixed state can always be interpreted as a subsystem of an entangled state where one of the degrees of freedom has been traced out. Even though there has been previous works on decoherence process simulations [32], we can generate a mixed state qubit with arbitrary degree of purity (i.e. Bloch vector norm) by performing a two-qubit operation with a single additional degree of freedom represented by the *environment* qubit. By applying a rotation along the Y-axis in Bloch sphere, implemented by the operator R_{env}, followed by a $CNOT$ operation, the *test* qubit suffers a decrease in its Bloch vector norm as the rotation introduced by R_{env} is changed from 0 to $\pi/2$ radians. Moreover, an additional unitary operator R_{prep} is applied, thus enabling the scheme to generate an arbitrary mixed state.

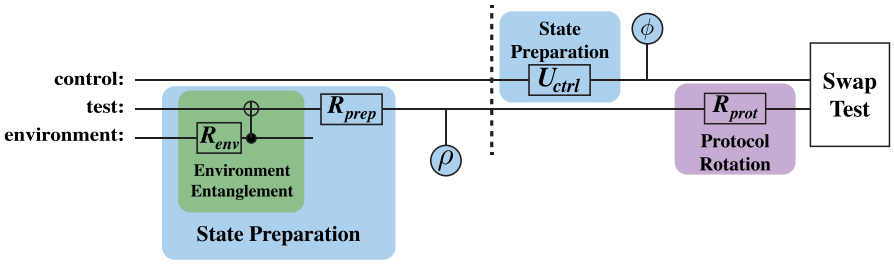

Fig. 4 Configuration for Swap Test Experiments. The structures on the left side of the dashed line correspond to the preparation procedure of an arbitrary *test* qubit, represented by the density operator ρ

Following DiVincenzo's criteria [33], we assume all qubits are initialized in the $|0\rangle$ state, as usual. The density operators ϕ and ρ correspond, respectively, to the *control* and *test* qubits immediately before the application of the "protocol rotation" R_{prot}, which will be explained further. The two inputs of the ST, therefore, will be given by the density operators ϕ and $R_{prot}\rho R_{prot}^{\dagger}$, where ϕ and ρ are given by:

$$\begin{aligned}\phi &= U_{ctrl}|0\rangle\langle 0|U_{ctrl}^{\dagger} \\ \rho &= R_{prep}\left[\mathrm{Tr}_{env}\left(U_{CNOT}(I\otimes R_{env})|0\rangle_{test}|0\rangle_{env}\langle 0|_{test}\langle 0|_{env}(I\otimes R_{env}^{\dagger})U_{CNOT}\right)\right]R_{prep}^{\dagger}\end{aligned} \tag{4}$$

where in the second line of Eq. 4 the term Tr_{env} means the partial trace over the *environment* qubit and U_{CNOT} is the controlled-NOT operation with the *test* qubit as the target.

2.2 Swap Test decoherence characterization challenges

Now we need to verify whether the scheme of Fig. 4 is able to tell apart a mixed state from a pure state. For this purpose, the idea is performing the ST for several different unitary transformations of the state ρ, which can be achieved by varying R_{prot}. This is similar to the varying observables that are measured in a standard quantum state tomography scenario.

In our simulations, we performed several ST iterations varying the R_{env} and R_{prot} operators. For each R_{env} rotation angle, that ranged from 0 to $\frac{\pi}{2}$ radians, we increased R_{prot} from 0 to π radians. As it is expected, the *test* and *environment* qubits become more entangled as R_{env} gets closer to $\frac{\pi}{2}$ radians and with that, the *test* qubit loses its purity, as seen in Fig. 5. Then, the unitary operation R_{prep} is adjusted to three different values, such that the *test* qubit ρ initially corresponds to the pure states $|0\rangle$, $|+i\rangle$ or $|+\rangle$. The *control* qubit is always set as either $|+\rangle$ or equal to the initial value of the *test* qubit along this simulation. Also, we analysed the differences when the R_{prot} operation corresponding to rotations along the Y-axis or X-axis.

Unfortunately, our experiments show that the results of the ST are not unique for each input qubit, regardless of the chosen ST variant (CSWAP or BSM). First, the purity of the *test* state did not influence the probability of obtaining output "1" in the

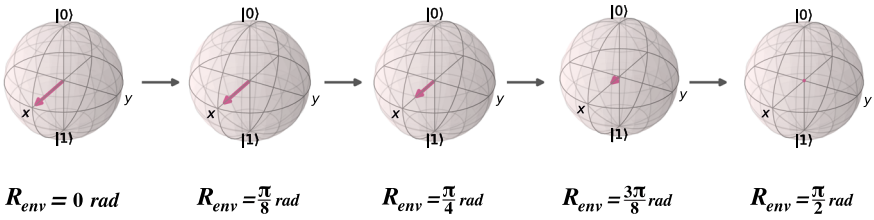

Fig. 5 Bloch sphere representation of the *test* qubit after the CNOT operation according to R_{env}, when it is initially set to the state $|+\rangle$. The purity of the state varies from 1 to 0

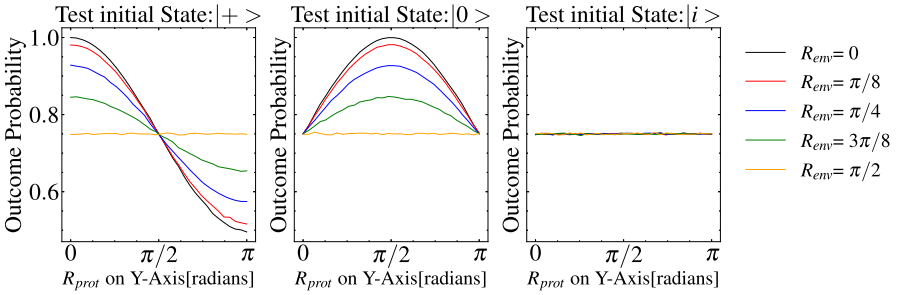

Fig. 6 Decoherence Characterization iteration using the Swap Test with *control* qubit set to $|+\rangle$ and R_{prot} set on the Y-axis. In this example, the CSWAP configuration was used; similar results are obtained for the BSM variation

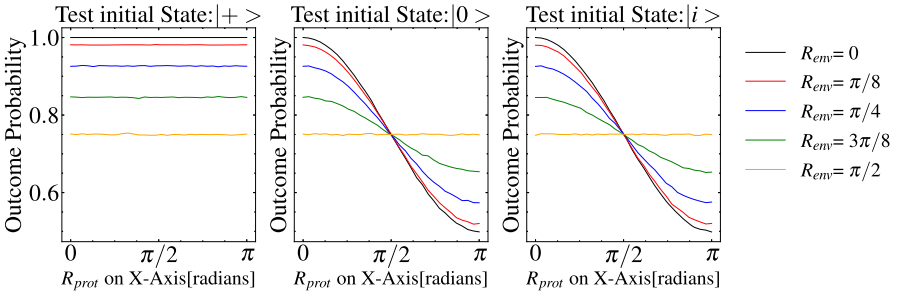

Fig. 7 Decoherence characterization iteration using the Swap Test where the *control* qubit state equals the *test* qubit initial state and R_{prot} performs rotations along the X-axis. In this example, the BSM configuration was used; similar results are obtained for the CSWAP variation

ST whenever it was initialized as $|+i\rangle$, as seen in Fig. 6. This means that any state lying along the Y-axis in Bloch sphere would produce the same result. As the rotation is being performed precisely around the Y-axis, one may be tempted to say that a change of axis would suffice to eliminate this redundancy; but it is not the case, as presented in Fig. 7, which now performs rotations along the X-axis. In this new scenario, results from initial states $|0\rangle$ and $|+i\rangle$ are now indistinguishable. Similar results are obtained when rotating along the Z-axis. It should be mentioned that the results shown in Figs. 6 and 7 are very similar in both ST variations (CSWAP and BSM). Thus, the proposed scheme in Fig. 4 cannot be used to characterize a decoherence process and distinguish its results for different states.

3 Swap Test with control measurement

Amid these shortcomings from the original ST, we proposed an adaptation to our initial ST protocol (Fig. 4). As our main goal was to characterize a decoherence process on a single qubit which we called *test* by performing the ST with another qubit labelled *control*, we decided to obtain the *control* measurement in parallel with the ST outcome, leaving the *test* qubit unobserved. We aimed to extract more information from the *test*

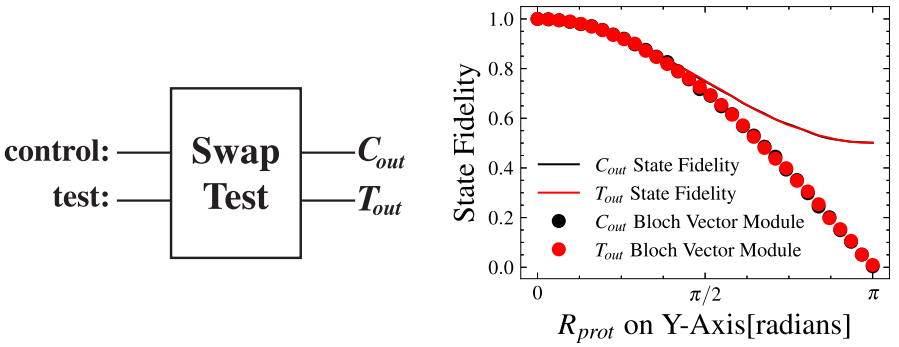

Fig. 8 State fidelity and state purity (Bloch vector norm) from Control and Test's states after undergoing the Swap Test (C_{out} and T_{out}). Fidelities are with respect to the corresponding inputs

Fig. 9 BSM ST translation into the Toffoli ST

qubit by analysing the ST result along with the *control* qubit measurement outcome. This decision was made owning to the fact that some ST configurations conserve both *test* and *control* qubits if their states overlap. Such fact has been highlighted in [28] and can be seen in Fig. 8 where we calculated the state fidelity of both qubits after the ST(C_{out} and T_{out}, corresponding to control and test, respectively) in comparison with their initial state. As seen, as the *control* and *test* qubits' states become closer to being orthogonal, they start losing fidelity to their initial state before the ST.

The state fidelity [34] is a metric that shows how close two quantum states are. Those states should be represented as density matrices and their fidelity can be found in Eq. 5. As seen, in order to calculate their fidelity, the density matrix from both states is needed. Being C_{out} and T_{out} unknown, we estimated their density matrices realizing a quantum state tomography (QST) procedure [34], a method for determining the density matrix of a state given a large number of its copies, represented in Eq. 6, where σ and ρ are generic density matrices between which one wishes to calculate the fidelity, and (X, Y, Z) are the Pauli spin operators. The traces in Eq. 6 are the experimental results one obtains when performing standard quantum state tomography.

$$F(\rho, \sigma) \equiv \mathrm{Tr}\sqrt{\rho^{1/2}\sigma\rho^{1/2}} \tag{5}$$

$$\rho = \frac{I + \mathrm{Tr}(X\rho)X + \mathrm{Tr}(Y\rho)Y + \mathrm{Tr}(Z\rho)Z}{2} \tag{6}$$

However, as previously seen, the BSM ST requires a measurement on both *test* and *control* qubits. Therefore, we decided to use the ST adaptation for the BSM ST previously presented by Cincio et al [27] where the measurements along with the post-measurement processing were substituted by a Toffoli gate which had as target an auxiliary (ancilla) qubit, as presented in Fig. 9. We referred to this ST modification as the Toffoli ST.

Furthermore, as we would be working with two measurements - on the *control* qubit and on the *ancilla* qubit in both Toffoli and CSWAP Swap Tests - a post-measurement processing was needed, as we are not merely extracting the measurement of two qubits anymore. On that premise, observing Fig. 4, if the *control* qubit, which is initially always equal to $|0\rangle$ before the start of any execution, is set to a desired state $|\phi\rangle$ by an unitary operation U, its adjoint $U^\dagger$ can be added right after the operations for a measurement on the $\{|\phi\rangle, |\phi^\perp\rangle\}$ basis. From this measurement, it is possible to detect whether the *control* qubit $|\phi\rangle$ was altered during the ST, by being different from *test* qubit, if $Prob(ctrl = 1) > 0$. That being said, as an outcome 1 on both *ancilla* or *control* qubit measurements yields distinguishable states, our post-measurement processing (see Fig. 9) is represented by a logic OR operation on both measurements, i.e. the measurement outcome equals 1 whenever the control qubit or the ancilla qubit (ST output) are equal to one. In other words, the measurement result only outputs a "0" when both its inputs are also "0", which creates a strict requirement for the output of the proposed methodology. Although it is rather difficult to grasp how much information is added to the output when this operation is performed, it lifts the degeneracy of the outputs of the original Swap Test, as presented and discussed in the next section. This allows the distinction between states with different levels of purity, otherwise not possible with the original Swap Test.

3.1 Decoherence characterization using the Toffoli Swap Test

Having our modification for the ST protocol, we tested both CSWAP and Toffoli Swap Tests with a *control* measurement in a decoherence scheme such as the one in Fig. 5, in order to check for improvements in the characterization process. Analysing our results, we found one iteration where it was possible to outline a decoherence process without any of the previously reported issues in Figs. 6 and 7.

The capability of the Toffoli ST with a *control* measurement to characterize an unknown quantum process can be demonstrated by the following calculations, considering the circuit presented in Fig. 4, with the Toffoli ST setting and assuming a rotation ϵ for Ry_{env}, where $0 \leq \theta \leq \frac{\pi}{2}$ and a protocol rotation α on Rx_{prot}. Let us consider the initial joint state $|init\rangle = |0\rangle_{env}|0\rangle_{test}|0\rangle_{ctrl}$ representing the environment, test and control qubits. The environment qubit undergoes a rotation $Ry_{env}(\epsilon)$ before a CNOT operation with the test qubit, which was initialized with the $R_{prep} = 0$, followed by the protocol rotation $Rx_{prot}(\alpha)$, whereas the control qubit undergoes a Hadamard operation ($U_{ctrl} = H$), resulting in the following joint state:

$$\begin{aligned}&\left[\cos\left(\frac{\varepsilon}{2}\right)\cos\left(\frac{\alpha}{2}\right)|0\rangle_{env}|0\rangle_{test} - i\cos\left(\frac{\varepsilon}{2}\right)\sin\left(\frac{\alpha}{2}\right)|0\rangle_{env}|1\rangle_{test}\right.\\&\left.-i\sin\left(\frac{\varepsilon}{2}\right)\sin\left(\frac{\alpha}{2}\right)|1\rangle_{env}|0\rangle_{test} + \sin\left(\frac{\varepsilon}{2}\right)\cos\left(\frac{\alpha}{2}\right)|1\rangle_{env}|1\rangle_{test}\right]\\&\otimes\left(\frac{1}{\sqrt{2}}|0\rangle_{ctrl} + \frac{1}{\sqrt{2}}|1\rangle_{ctrl}\right)\end{aligned}$$

This state can be simplified to:

$$\begin{aligned}
&\frac{1}{2}\cos\left(\frac{\varepsilon}{2}\right) e^{-i\frac{\alpha}{2}}|0,0,0\rangle + \frac{1}{2}\cos\left(\frac{\varepsilon}{2}\right) e^{i\frac{\alpha}{2}}|0,0,1\rangle \\
&+\frac{1}{2}\cos\left(\frac{\varepsilon}{2}\right) e^{-i\frac{\alpha}{2}}|0,1,0\rangle - \frac{1}{2}\cos\left(\frac{\varepsilon}{2}\right) e^{i\frac{\alpha}{2}}|0,1,1\rangle \\
&+\frac{1}{2}\sin\left(\frac{\varepsilon}{2}\right) e^{-i\frac{\alpha}{2}}|1,0,0\rangle - \frac{1}{2}\sin\left(\frac{\varepsilon}{2}\right) e^{i\frac{\alpha}{2}}|1,0,1\rangle \\
&+\frac{1}{2}\sin\left(\frac{\varepsilon}{2}\right) e^{-i\frac{\alpha}{2}}|1,1,0\rangle + \frac{1}{2}\sin\left(\frac{\varepsilon}{2}\right) e^{i\frac{\alpha}{2}}|1,1,1\rangle
\end{aligned}$$

where the notation $|x, y, z\rangle$ was used instead of $|x\rangle_{env}|y\rangle_{test}|z\rangle_{ctrl}$.

Now, we introduce the ancilla qubit and use this state as the input to the Toffoli gate. At the output of the latter, a Hadamard gate is applied to the control qubit rail; we are only interested (due to the OR gate defined in Eq. (6)) in the cases where both control and ancilla are in the $|0\rangle$ state. Therefore, we post-select the components where this is true and obtain the following (post-selected) output state after a straightforward but somewhat lengthy calculation:

$$\begin{aligned}
|out\rangle = &\frac{1}{\sqrt{2}}\cos\left(\frac{\varepsilon}{2}\right)\cos\left(\frac{\alpha}{2}\right)|0,0,0,0\rangle + \frac{1}{2\sqrt{2}}\cos\left(\frac{\varepsilon}{2}\right) e^{-i\frac{\alpha}{2}}|0,1,0,0\rangle \\
&-\frac{1}{\sqrt{2}}\sin\left(\frac{\varepsilon}{2}\right)\sin\left(\frac{\alpha}{2}\right)|1,0,0,0\rangle + \frac{1}{2\sqrt{2}}\sin\left(\frac{\varepsilon}{2}\right) e^{-i\frac{\alpha}{2}}|1,1,0,0\rangle,
\end{aligned}$$

where the last qubit is the ancilla qubit. The probability associated to this event can be calculated as:

$$\begin{aligned}
Prob(0,0) =& \frac{1}{2}\cos^2\left(\frac{\varepsilon}{2}\right)\cos^2\left(\frac{\alpha}{2}\right) + \frac{1}{8}\cos^2\left(\frac{\varepsilon}{2}\right) \\
&+ \frac{1}{2}\sin^2\left(\frac{\varepsilon}{2}\right)\sin^2\left(\frac{\alpha}{2}\right) + \frac{1}{8}\sin^2\left(\frac{\varepsilon}{2}\right) \\
=& \frac{3}{8} + \frac{1}{4}(\cos(\varepsilon)\cos(\alpha)).
\end{aligned}$$

This calculation result can be verified by the performed simulations, as presented in Fig. 10, where we also added the plots for all of the orthogonal states of the original ones. Note that states $|+\rangle$ and $|-\rangle$ lie along the X-axis, and therefore $R_{prot}(\alpha)$ has no effect on the outcome probability. In fact, a similar calculation shows that, for states alongside the X-axis, the probability of success for a modified Toffoli ST is given by:

$$Prob(0,0) = \frac{3}{8} \pm \frac{1}{8}\cos(\varepsilon),$$

where the sign is positive (negative) for states closer to $|+\rangle$ ($|-\rangle$).

With that said, this protocol setting, presented in Fig. 11, was able to both distinguish results for our test cases and demonstrate unique curves according to how the *test* qubit was affected by decoherence. As we have tested for all of the Pauli matrices eigenstates,

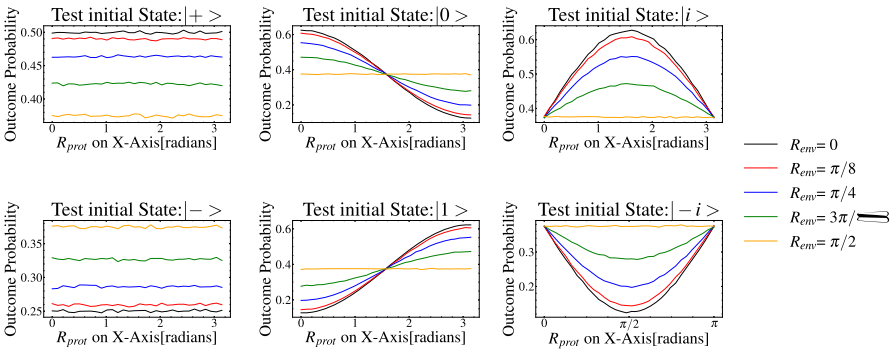

Fig. 10 Decoherence Characterization iteration using the Toffoli ST with a *control* qubit measurement, having the control qubit's state set to $|+\rangle$ and R_{prot} set on the X-axis

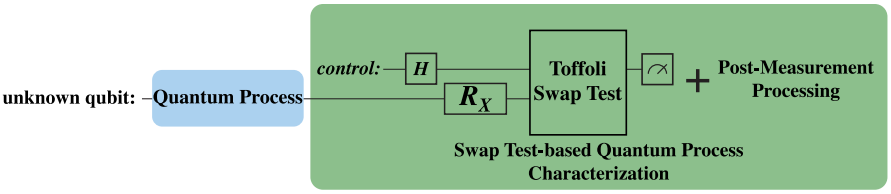

Fig. 11 Swap Test-based workflow for decoherence characterization with the following steps: (1) apply decoherence to an unknown qubit; (2) prepare the unknown qubit with a rotation on the X-axis (R_X) and the control qubit with a Hadamard gate H; (3) perform the Toffoli Swap Test, as disclosed in Sect. 3, where an ancilla qubit is included but only relevant to the Swap Test; (4) perform the necessary measurements with the control and ancilla qubit; (5) perform a post-measurement data processing final step, corresponding to a logic OR operation between the ancilla and control qubit measurement results

this method is valid for any state on the Bloch sphere. Interestingly enough, note that the method only employs unitary operations that correspond to rotations around the X-axis; in other words, we measure observables that correspond to axes belonging to a great circle on Bloch sphere that connects the poles and pass through the states $|+i\rangle$ and $|-i\rangle$.

It should be noted that, according to Fig. 10, as long as the input state is known except for its Bloch vector length, only one angle value is needed in order to find it out; except for angles 0, $\pi/2$ and π (where the lines intersect in some cases), an analysis at any other angle would suffice, because a single point determines the full curve. This means that, in this particular scenario, no actual "rotation" is needed, i.e. the method employs a static quantum circuit, in the same way as in a standard quantum state tomography.

4 Comparing Swap Test circuit variants on real quantum computers

Up to this point, we have employed Qiskit's Aer *qasm_simulator* backend [29]; the next natural step is running a test bench for the ST variants on a real IBM quantum computer, in order to analyse the innate decoherence which is present in every quantum

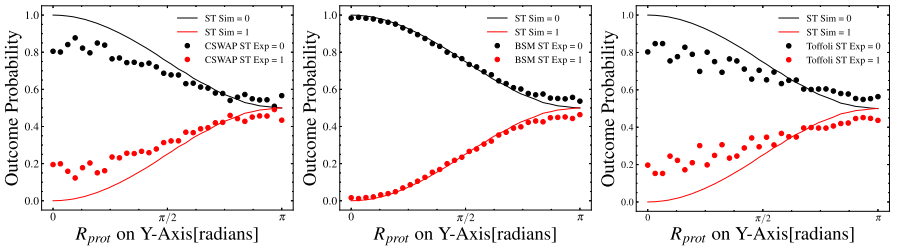

(a) Original Swap Test results (b) BSM Swap Test results (c) Toffoli Swap Test results

Fig. 12 Swap Test's outcomes on a real IBM quantum computer - the *ibmq_manila*. The plots distinguish the simulation results (lines) from the actual experimental ones (dots). It can be seen that the BSM ST produces results that are much closer to the simulation results, when compared to the CSWAP ST and Toffoli Swap Tests

computer. This natural decoherence is due to the natural (unwanted) coupling between the qubits and the environment, which increases with the circuit depth.

In order to verify whether practical quantum computers have noticeable decoherence effects, even for short quantum circuits, we realized an experiment in which both *test* and *control* qubits were initially prepared at the $|+\rangle$ state, without any "artificial" decoherence process, with R_{env} set to 0. The *test* qubit was gradually rotated along the Y-axis by the R_{prot} operation while the *control* qubit remained unchanged. The *test* qubit was rotated until the $|-\rangle$ state, where it would be orthogonal to the *control* qubit's state.

The final measurements presented in Fig. 12 have been performed in the quantum computer *ibmq_manila*, during a period of 1 week. For each Swap Test characterization run, we measured 4 observables at 32 different rotation settings, each of which running at 8192 repetitions, amounting to over 900 thousand measurement runs for each configuration of the Swap Test (original, BSM, and Toffoli). These extensive results indicate that the decoherence intrinsic to the *ibmq_manila* architecture is not appropriate for the evaluation of the proposed Swap Test-based decoherence characterization, since the process itself suffers from the short comings of the quantum computer. However, it is clear that the BSM ST provides a better experimental output. This is related to the practical implementation of the Toffoli gate, which (in practice) is obtained by combining many CNOTs and elementary one-qubit gates, whereas the BSM ST is comprised of a shorter circuit depth and requires less qubits and gates. New generations of quantum processors will soon match the performance required, enabling further tests of the proposed method in a real quantum computer.

5 Conclusion

The Swap Test has been investigated as an agnostic tool for characterization of decoherence in quantum computers. We have shown with simulations and experiments on an actual quantum computer from IBM that a simple comparison between a control and a test qubit using standard Swap Test schemes does not unveil enough information to determine with certainty whether the test qubit has suffered decoherence, i.e.

if it's in a mixed state. A modified version of the Toffoli Swap Test, on the other hand, can be employed for successfully characterizing a decoherence process on a qubit, by performing the Swap Test between a known pure state (control) and a mixed state (test), where the latter is obtained by a controlled entanglement with an auxiliary qubit (environment). The procedure lacks the generality of standard quantum process tomography, but involves the measurement of fewer observables and enables the possibility of assessing the indistinguishability of the input states. Moreover, it has the possible advantage of not destroying the test qubit in the process, even though it is not kept unmodified in the case where decoherence takes place. Possible reuse of the information remaining in the output states needs further investigation. We expect this work might result in new investigations on the applicability of the Swap Test in quantum computer characterizations.

It should be mentioned that the full power of the Swap Test cannot be achieved unless we have access to internal degrees of freedom of the qubit, as happens for example in a Hong-Ou-Mandel interferometer with photonic qubits, which enables us to distinguish time-varying unitary operations from actual decoherence (i.e. entanglement with the environment). This examination will be performed in a future work.

Acknowledgements The authors acknowledge the financial support of CAPES, CNPq and FAPERJ.

Data availability The data sets generated during and/or analysed during the current study are available from the corresponding author on reasonable request.

Declarations

Conflict of interest The authors declare that they have no conflict of interest.

References

1. Preskill, J.: Quantum computing in the NISQ era and beyond. Quantum **2**, 79 (2018)
2. Eisert, J., Hangleiter, D., Walk, N., Roth, I., Markham, D., Parekh, R., Chabaud, U., Kashefi, E.: Quantum certification and benchmarking. Nat. Rev. Phys. **2**, 382–390 (2020)
3. ...Wright, K., Beck, K.M., Debnath, S., Amini, J.M., Nam, Y., Grzesiak, N., Chen, J.S., Pisenti, N.C., Chmielewski, M., Collins, C., Hudek, K.M., Mizrahi, J., Wong-Campos, J.D., Allen, S., Apisdorf, J., Solomon, P., Williams, M., Ducore, A.M., Blinov, A., Kreikemeier, S.M., Chaplin, V., Keesan, M., Monroe, C., Kim, J.: Benchmarking an 11-qubit quantum computer. Nat. Commun. **10**, 5464 (2019)
4. Knill, E., Leibfried, D., Reichle, R., Britton, J., Blakestad, R.B., Jost, J.D., Langer, C., Ozeri, R., Seidelin, S., Wineland, D.J.: Randomized benchmarking of quantum gates. Phys. Rev. A **77**, 012307 (2008)
5. Helsen, J., Roth, I., Onorati, E., Werner, A.H., Eisert, J.: A general framework for randomized benchmarking. PRX Quant. **3**(2), 020357 (2020)
6. Xue, X., Watson, T.F., Helsen, J., Ward, D.R., Savage, D.E., Lagally, M.G., Coppersmith, S.N., Eriksson, M.A., Wehner, S., Vandersypen, L.M.K.: Benchmarking gate fidelities in a Si/SiGe two-qubit device. Phys. Rev. X **9**, 021011 (2019)
7. Cross, A.W., Bishop, L.S., Sheldon, S., Nation, P.D., Gambetta, J.M.: Validating quantum computers using randomized model circuits. Phys. Rev. A **100**, 032328 (2019)
8. Hradil, Z.: Quantum-state estimation. Phys. Rev. A **55**, 1561–1564 (1997)
9. James, D.F.V., Kwiat, P.G., Munro, W.J., White, A.G.: Measurement of qubits. Phys. Rev. A **64**, 052312 (2001)
10. Kalev, A., Kosut, R., Deutsch, I.: Quantum tomography protocols with positivity are compressed sensing protocols. NPJ Quant. Inf. **1**, 15018 (2015)

11. Baumgratz, T., Gross, D., Cramer, M., Plenio, M.B.: Scalable reconstruction of density matrices. Phys. Rev. Lett. **111**, 020401 (2013)
12. Torlai, G., Mazzola, G., Carrasquilla, J.E.A.: Neural-network quantum state tomography. Nat. Phys. **14**, 447 (2018)
13. Proctor, T., Seritan, S., Rudinger, K., Nielsen, E., Blume-Kohout, R., Young, K.: Scalable randomized benchmarking of quantum computers using mirror circuits. Phys. Rev. Lett. **129**, 150502 (2022)
14. Harper, R., Flammia, S.T., Wallman, J.J.: Efficient learning of quantum noise. Nat. Phys. **16**, 1184–1188 (2020)
15. Zhang, Y., Yu, W., Zeng, P., Liu, G., Ma, X.: Scalable fast benchmarking for individual quantum gates with local twirling. Photon. Res. **11**(1), 81 (2023)
16. Xavier, G.B., Temporão, G.P., von der Weid, J.P.: Quantum channel with controllable decoherence using polarization-time coupling. Eur. Phys. J. D **66**, 42 (2012)
17. Amaral, G.C., Carneiro, E.F., Temporão, G.P., von der Weid, J.P.: Complementarity analysis of interference between frequency-shifted photonic wave packets. JOSA B **35**(3), 601 (2018)
18. Hong, C.K., Ou, Z.Y., Mandel, L.: Measurement of subpicosecond time intervals between two photons by interference. Phys. Rev. Lett. **59**, 2044 (1987)
19. Buhrman, H., Cleve, R., Watrous, J., de Wolf, R.: Quantum Fingerprinting. Phys. Rev. Lett. **87**(16), 167902 (2001)
20. Garcia-Escartin, J.C., Chamorro-Posada, P.: Swap test and Hong-Ou-Mandel effect are equivalent. Phys. Rev. A **87**(5), 052330 (2013)
21. Consiglio, M., Apollaro, T.J.G., Wieśniak, M.: Variational approach to the quantum separability problem. Phys. Rev. A **106**, 062413 (2022)
22. Das, S., Zhang, J., Martina, S., Suter, D., Caruso, F.: Quantum pattern recognition on real quantum processing units. Quant. Mach. Intell. **5**(1), 16 (2023)
23. Volkoff, T.J., Subaşı, Y.: Ancilla-free continuous-variable SWAP test. Quantum **6**, 800 (2022)
24. Li, Y.D., Barraza, N., Alvarado Barrios, G., Solano, E., Albarrán-Arriagada, F.: Swap test with quantum dot charge qubits. Phys. Rev. Appl. **18**, 014047 (2022)
25. Nguyen, C.H., Tseng, K.W., Maslennikov, G., Gan, H.C.J., Matsukevich, D.: Experimental swap test of infinite dimensional quantum states (2021)
26. Chapman, B.J., de Graaf, S.J., Xue, S.H., Zhang, Y., Teoh, J., Curtis, J.C., Tsunoda, T., Eickbusch, A., Read, A.P., Koottandavida, A., Mundhada, S.O., Frunzio, L., Devoret, M.H., Girvin, S.M., Schoelkopf, R.J.: A high on-off ratio beamsplitter interaction for gates on bosonically encoded qubits (2022)
27. Cincio, L., Subaşı, Y., Sornborger, A.T., Coles, P.J.: Learning the quantum algorithm for state overlap. New J. Phys. **20**(11), 113022 (2018)
28. Foulds, S., Kendon, V., Spiller, T.: The controlled swap test for determining quantum entanglement. Quant. Sci. Technol. **6**(3), 035002 (2021)
29. H.A. *et al*.: Qiskit: An open-source framework for quantum computing (2019)
30. Peres, A.: Quantum theory: concepts and methods. Kluwer Academic Publishers, The Netherlands (1995)
31. Wang, Q., Zhang, Z., Chen, K., Guan, J., Fang, W., Liu, J., Ying, M.: Quantum algorithm for fidelity estimation. IEEE Trans. Inf. Theory **69**(1), 273–282 (2022)
32. Heusler, S., Dür, W.: Modeling decoherence with qubits. Eur. J. Phys. **39**(2), 025406 (2018)
33. DiVincenzo, D.P.: The physical implementation of quantum computation. Fortschritte der Physik **48**(9–11), 771 (2000)
34. Nielsen, M.A., Chuang, I.L.: Quantum computation and quantum information: 10th anniversary edition, 10th edn. Cambridge University Press, USA (2011)